

## Phosphine $\pi$ -Acceptor Properties in Dihalogenobis(triphenylphosphine)-nickel(II) and -cobalt(II)

By John E. Davies, Malcolm Gerloch,\* and David J. Phillips, University Chemical Laboratory, Lensfield Road, Cambridge CB2 1EW

Principal paramagnetic susceptibilities of single crystals of  $[ML_2X_2]$  ( $M = Ni$  or  $Co$ ;  $L =$  triphenylphosphine;  $X = Cl$  or  $Br$ ) have been measured by the Faraday method throughout the temperature range 20–300 K. The magnetic properties, together with literature spectral data from single crystals and powders, have been interpreted within the angular overlap model (a.o.m.). No symmetry idealizations have been made. Fitting regions within the parametric models are broad but there emerges an unambiguous conclusion that large, negative, a.o.m. parameters are to be associated with the phosphine ligands in all cases. This evidence for  $\pi$ -acid behaviour for these ligands is associated with the observation of large nephelauxetic effects in these systems.

THAT phosphines adopt a  $\pi$ -acceptor role within their bonding to transition-metal ions has long been supposed. Evidence for a synergic  $d_{\pi}$ - $d_{\pi}$  contribution to metal-phosphine bonding appears to have been indirect, being based upon the facility with which phosphines can replace carbonyl groups in many complexes, kinetic and thermodynamic phenomena groups within the 'trans effect,' and on occasion by reference to certain n.m.r. coupling constants.<sup>1</sup> Recently, however, Mason and Meek<sup>1</sup> have argued that, within a series of platinum and palladium phosphine species at least, there is no structural evidence in support of any significant role for such  $\pi$  bonding, their conclusion being based upon the interpretation of bond lengths from accurate X-ray structural analyses within the concepts of bond hybridization and additivity.

Several advances<sup>2</sup> in the techniques of magnetochemistry made over the last few years have conferred upon the method a real possibility of making meaningful commentary on the relative roles of  $\sigma$  and  $\pi$  bonding in transition-metal complexes. In particular, studies of paramagnetism can furnish angular-overlap parameters relating to local metal-ligand bonding symmetry in a way that is at least complementary to, and often more sensitive than, the technique of electronic absorption spectroscopy. We describe here a study of the single-crystal magnetic susceptibilities and of some polarized single-crystal electronic spectra of four molecules:  $[ML_2X_2]$ , where  $M = Co^{II}$  or  $Ni^{II}$ ,  $L =$  triphenylphosphine, and  $X = Cl$  or  $Br$ . In addition to exploring further the behaviour of modern magnetochemical techniques, the study appears to furnish more direct evidence of a significant  $\pi$ -acid role for the triphenylphosphine ligands in these systems whether or not this is associated with a shortening of the metal-phosphorus bond lengths from some defined norm.

### EXPERIMENTAL

The compounds  $[M(PPh_3)_2X_2]$  ( $M = Ni$  or  $Co$ ;  $X = Cl$  or  $Br$ ) were prepared using methods described by Venanzi.<sup>3</sup> Well formed single crystals (2–10 mg) were obtained by recrystallization from a mixture of n-butanol and 1,2-dimethoxypropane in a vacuum desiccator. X-Ray rotation and Weissenberg photographs were used to examine and orientate the crystals.

The compounds  $[CoL_2Cl_2]$ ,  $[CoL_2Br_2]$ , and  $[NiL_2Br_2]$  can all be crystallized with the  $[NiL_2Cl_2]$  structure ( $L = PPh_3$ )<sup>4</sup> (see Figure 1). Some care is required with  $[NiL_2Br_2]$  because crystalline samples of this material may contain two (and possibly three) different crystal forms. Fortunately, the two major forms are readily distinguished

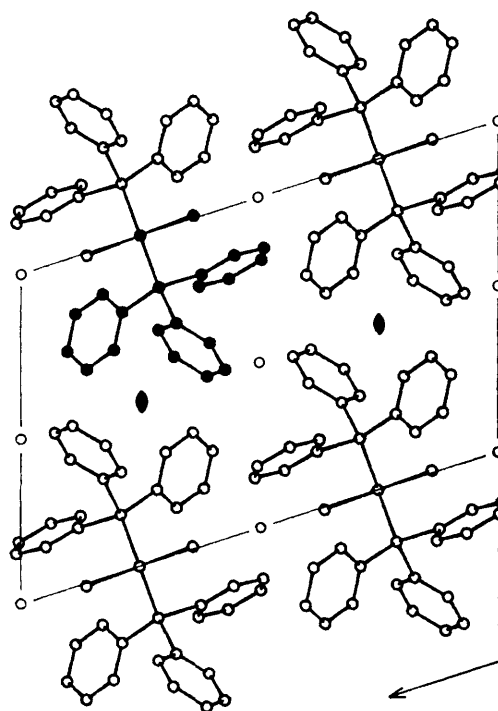


FIGURE 1. The structure of  $[Ni(PPh_3)_2Cl_2]$ : space group  $P2_1/c$ ,  $a = 11.70$ ,  $b = 8.31$ ,  $c = 17.59$  Å,  $\beta = 108^\circ$  (ref. 4). The  $b$  axis is perpendicular to the page, the asymmetric unit being indicated by filled circles. Molecules with the metal atom at  $y = \frac{1}{4}$  are related to molecules with  $y = \frac{3}{4}$  by inversion centres

from each other. Crystals isomorphous with  $[NiL_2Cl_2]$  are rectangular prisms (see Figure 2); the other, more abundant form, occurs as needle-shaped prisms and has a  $P2_1/c$  structure with  $a = 37.2$  Å.<sup>5</sup> All data reported here were obtained from crystals with the  $P2_1/c$   $[NiL_2Cl_2]$  structure (Figure 1).

Single-crystal magnetic susceptibilities in the temperature range 20–295 K were measured with the Faraday balance described by Cruse and Gerloch.<sup>6</sup> Interpolated principal susceptibilities are listed in Table 1. The crystal

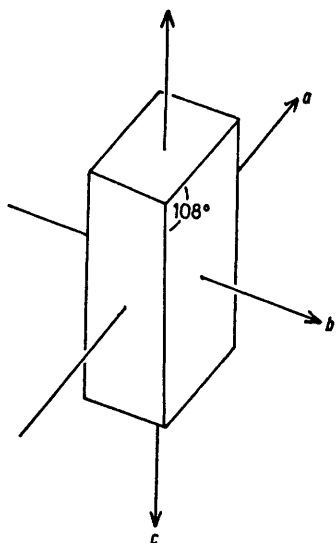
TABLE 1

Principal crystal (molecular) susceptibilities for  $[ML_2X_2]$  ( $M = Ni$  or  $Co$ ;  $X = Cl$  or  $Br$ )

$T/K$	$[Ni(PPh_3)_2Cl_2]$			$[Ni(PPh_3)_2Br_2]$			$[Co(PPh_3)_2Cl_2]$			$[Co(PPh_3)_2Br_2]$		
	$\chi_c$	$\chi_{a^*}$	$\chi_b$	$\chi_c$	$\chi_{a^*}$	$\chi_b$	$\chi_{a^*}$	$\chi_c$	$\chi_b$	$\chi_{a^*}$	$\chi_c$	$\chi_b$
20	371	643	611	461	522	583	515	1 867	602	618	1 797	594
	396	628	670	411	597	702	651	1 927	471	673	1 899	492
35	260	370	360	292	316	347	418	986	459	472	976	456
	267	355	371	272	343	384	481	977	391	490	960	401
55	180	232	228	199	209	223	313	571	331	343	575	334
	183	223	231	185	218	238	342	563	297	346	555	302
75	139	171	167	156	160	164	247	396	255	275	412	259
	138	163	168	140	160	172	263	390	236	265	385	238
95	111	132	130	123	126	130	201	300	205	225	323	213
	111	128	132	112	126	135	213	297	194	214	293	196
115	94	110	107	101	103	106	171	243	174	177	254	179
	93	106	108	94	104	111	178	240	165	179	237	166
135	81	94	92	87	88	91	148	204	151	145	206	154
	80	90	92	80	89	94	154	201	143	154	198	144
155	71	82	80	76	77	79	131	176	133	137	180	136
	70	78	80	71	78	82	135	172	127	135	171	127
175	64	73	72	67	68	71	117	155	118	124	159	122
	62	69	71	63	69	73	120	151	113	121	150	114
195	58	65	65	61	62	64	106	139	107	111	142	111
	56	62	64	57	62	65	108	135	103	109	133	103
215	53	60	59	56	56	58	97	126	98	102	129	101
	51	57	58	52	56	59	99	121	94	99	120	94
235	48	55	54	51	52	53	90	115	90	94	118	93
	47	52	53	47	51	54	91	111	86	91	110	87
255	44	50	50	47	48	49	83	106	83	88	109	86
	43	48	49	44	48	50	84	102	80	84	101	80
275	41	47	46	44	45	46	78	99	77	82	101	80
	40	44	45	41	44	47	78	94	75	78	93	75
295	39	44	44	41	42	43	73	92	72	77	94	75
	38	41	42	38	41	44	73	87	70	73	87	70

$\chi/c.g.s. units \times 10^{-4}$  (1 c.g.s. unit =  $4\pi \times 10^{-6} m^3 mol^{-1}$ ). Observed and calculated values, respectively, are given vertically in each column. Calculated values derive from the parameter sets given in Table 7. In each case, the orientations of  $\chi_1$  and  $\chi_2$  lie within  $3^\circ$  of  $a^*$  or  $c$ .

structure (Figure 1) is a particularly simple and convenient one for these measurements; the two possible molecular orientations (those with metal  $y$  co-ordinate either  $\frac{1}{4}$  or  $\frac{3}{4}$ ) are related by centres of symmetry. In this special mono-

FIGURE 2 Crystal morphology of  $[Ni(PPh_3)_2Cl_2]$ 

clinic case, the principal crystal susceptibilities are identical to the principal molecular susceptibilities (since magnetic susceptibility is a centrosymmetric physical property). Thus, one of the principal molecular susceptibilities ( $\chi_3 = \chi_b$ ) is parallel to the bisector of the angle  $X-M-X$ .

The orientation of  $\chi_2$  with respect to the crystal  $a$  and  $c$  axes was obtained in each case by observing the position of  $\chi_{max}$  in the  $ac$  plane relative to the (known) orientation of the crystal. For each of the four derivatives,  $\chi_1$  is parallel to either  $a^*$  or  $c$  ( $\chi_2$  parallel to either  $c$  or  $a^*$ ) within the experimental error ( $\pm 3^\circ$ ). These positions do not change measurably in the temperature range 20–295 K. Thus the directions of the two principal molecular susceptibilities in the  $ac$  plane are approximately parallel to the  $ac$  projections of the metal-halogen and metal-phosphorus bonds (see Figure 1). For the nickel derivatives,  $\chi_1 = \chi_c$ ,  $\chi_2 = \chi_{a^*}$  and for the cobalt derivatives,  $\chi_1 = \chi_{a^*}$ ,  $\chi_2 = \chi_c$  ( $\chi_1 < \chi_2$ ;  $\chi_3 = \chi_b$  by convention).

## DISCUSSION

We have the following data available for interpretation: (a) accurate single-crystal principal paramagnetic susceptibilities throughout the temperature range 20–295 K for all four complexes  $[ML_2X_2]$  ( $M = Ni^{II}$  or  $Co^{II}$ ;  $X = Cl$  or  $Br$ ;  $L = PPh_3$ ); (b) single-crystal polarized transmission spectra for the two chloro-complexes<sup>7,8</sup> and for  $[CoL_2Br_2]$ ;<sup>9</sup> (c) a diffuse-reflectance spectrum for  $[NiL_2Br_2]$ .<sup>10</sup> We shall describe the reproduction of these data by appropriate quantum-mechanical and magnetochemical models in sufficient detail to demonstrate that, despite an obvious spread of possible parameter values, there emerges an unambiguous conclusion concerning the role of metal-phosphorus  $\pi$  bonding.

*Parameters.*—Calculations of spectral and magnetic properties have been performed using the models and

techniques reported recently.<sup>6,11</sup> A basis spanning all free-ion terms of the same spin multiplicity as that of the ground term was used: for the nickel systems,  ${}^3F + {}^3P$ ; for cobalt,  ${}^4F + {}^4P$ . In all cases, the approximate molecular symmetry is  $C_{2v}$ , but no idealizing assumptions have been made in our calculations, ligands being placed at the positions determined by the X-ray structural analysis.<sup>4</sup> The co-ordination geometry is shown in Figure 3, together with the molecular cartesian axis frames adopted in this paper.

The behaviour of these models with respect to the following parameters will be described:  $B$ , Racah's interelectron repulsion parameter;  $e_\sigma(P)$ ,  $e_\sigma(X)$  for  $\sigma$  interactions between the metal and phosphine or halogen ligands respectively;  $e_\pi(P)$ ,  $e_\pi(X)$  for  $\pi$  interactions, presumed to be cylindrical with respect to each metal-

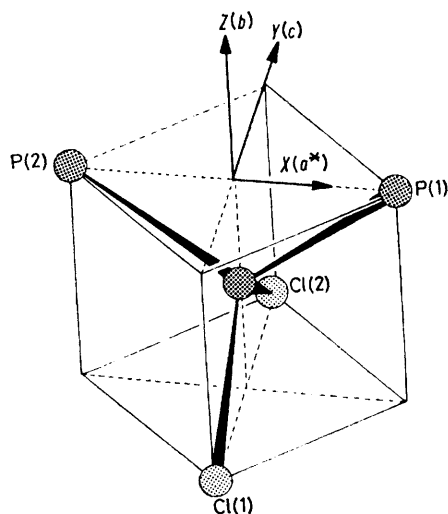


FIGURE 3 Relationships between crystallographic axes  $a^*$ ,  $b$ ,  $c$ , spectrum polarization axes  $X, Y, Z$ , and the idealized first co-ordination shell

ligand vector (for both phosphine and X ligands);  $\zeta$ , the one-electron spin-orbit coupling coefficient in the complex; and  $k$ , Stevens' orbital-reduction factor (only entering into the magnetic susceptibility calculations).

*Dichlorobis(triphenylphosphine)nickel(II)*.—We begin by considering what information may be obtained by fitting the magnetic data *alone*. Wide ranges for all parameters were investigated, readily yielding two main conclusions: that the 'fitting region' is broad and that  $e_\pi(P)$  is large and negative. Agreement between observed and calculated susceptibilities, for all three principal tensor components simultaneously, within *ca.* 6% is obtained with the following parameter values:  $B$  is ill defined, as expected;  $\zeta \sim 350 \pm 50 \text{ cm}^{-1}$ , compared with the free-ion value  $\zeta_0 = 630 \text{ cm}^{-1}$ ;  $k$ , not very sensitively defined, lies between 0.5 and 0.7;  $e_\sigma(P)$  and  $e_\sigma(Cl)$  may lie between 3 000 and 5 000  $\text{cm}^{-1}$  while  $e_\pi(P)$  lies between  $-1\,500$  and  $-5\,000 \text{ cm}^{-1}$  and  $e_\pi(Cl)$  between  $+1\,000$  and  $+3\,500 \text{ cm}^{-1}$  without significant correlation; a value of  $e_\pi(P)$  of *ca.*  $-1\,000 \text{ cm}^{-1}$  is possible when  $e_\pi(Cl) = +3\,000 \text{ cm}^{-1}$ . Zero or positive values for  $e_\pi(P)$

in conjunction with any values of the other parameters yield no acceptable agreement between observed and calculated magnetic properties. The negative values required for  $e_\pi(P)$  describe the essential conclusion to be deduced from the magnetic properties of  $[\text{NiL}_2\text{Cl}_2]$  alone. The qualitative nature of this conclusion is disappointing in relation to other more sensitively defined fits obtained recently for other systems. Nevertheless the qualitative validity seems assured by comparison with the success of the model for these other systems,<sup>2,6,12</sup> with the other 'tetrahedral' complexes discussed in this paper, and with the interpretation of the crystal spectrum which we now discuss.

Hathaway and his co-workers<sup>7</sup> have reported the crystal transmission spectrum of  $[\text{NiL}_2\text{Cl}_2]$  in polarized light. After due allowance for the change in reference frame used in ref. 7 to that in Figure 1, the main features of their spectrum are as follows: only one, rather weak, band in  $X$  polarization, at *ca.*  $8\,000 \text{ cm}^{-1}$ ; two bands in  $Z$  polarization at *ca.*  $18\,000$  and  $10\,200 \text{ cm}^{-1}$ ; four bands in  $Y$  polarization at *ca.*  $18\,000$ ,  $12\,000$ ,  $11\,200$ , and  $\lesssim 4\,800 \text{ cm}^{-1}$ . A further, relatively sharp, peak in  $Y$  polarization at *ca.*  $10\,800 \text{ cm}^{-1}$  seems certain to be assigned as the spin-forbidden  ${}^3B_1 \rightarrow {}^1E$  transition. Allowing for the band at *ca.*  $18\,000 \text{ cm}^{-1}$  occurring in both  $Y$  and  $Z$  polarization, therefore, there remain six bands which might reasonably be assigned as spin-allowed transitions. Assuming electric dipole selection rules, together with the idealized symmetry group  $C_{2v}$  in which all three principal directions can be expected to involve inequivalent spectral absorption, the earlier workers deduced a  ${}^3B_1$  ground term (using the axis frame in Figure 1). All fitting regions for the magnetic susceptibilities just described involve a formal  ${}^3B_1$  ground term in agreement with this. Accordingly we expect to observe transitions from  ${}^3B_1$  to  ${}^3A_1$  in  $X$  polarization, to  ${}^3A_2$  in  $Y$  polarization, and to  ${}^3B_1$  in  $Z$  polarization. Transitions to  ${}^3B_2$  are dipole forbidden. In  $C_{2v}$  symmetry a  $T_1(T_d)$  term transforms as  $A_2 + B_2 + B_1$ , a  $T_2(T_d)$  as  $A_1 + B_1 + B_2$ , and  $A_2(T_d)$  as  $A_2$ . We therefore expect two excited  ${}^3B_1$  terms, one  ${}^3A_1$ , and three  ${}^3A_2$  terms and hence we should observe six spin-allowed transitions. There follow the ready assignments  ${}^3B_1 \rightarrow {}^3A_1$  ( $8\,000 \text{ cm}^{-1}$ );  $\rightarrow {}^3A_2$  ( $\lesssim 4\,800$  and  $11\,200 \text{ cm}^{-1}$ );  $\rightarrow {}^3B_1$  ( $10\,200$  and  $18\,000 \text{ cm}^{-1}$ ). Provided this assignment can be reproduced quantitatively using reasonable parameter values in our model, there is no reason to look for more complex assignments involving singlet-triplet intensity-stealing processes and the like. We have fitted these transitions independently from the susceptibilities in the following way.

Eigenvalue calculations were again carried out within the real geometry of the complex (*i.e.* less than  $C_{2v}$  symmetry), including spin-orbit coupling. From the resulting eigenvectors, representations of  $C_{2v}$  were projected out using the relationship (1) where  $h$  is the order

$$P(\Gamma) = \frac{1}{h} \sum_S \chi(\Gamma, S) \langle \psi | S \psi \rangle \quad (1)$$

of the group,  $S$  is a symmetry operator of the group acting only upon the spatial parts of the wavefunctions, and  $P$  is the projector of the representation  $\Gamma$ . In this way, eigenfunctions could be assigned within the idealized  $C_{2v}$  group while spin-orbit-induced mixing between representations could be monitored at the same time. For a given parameter set, a figure of merit was assigned to each spectral band and an overall figure of merit was assigned to the set of bands according to the following empirical scheme. Each observed transition energy was assigned a 'band width' based upon the reported spectrum and corresponding to the half-width of the band at a quarter-height. Figures of merit ( $R$ ) were then calculated according to equation (2). In

$$R = 100 - 10[(E_{\text{obs.}} - E_{\text{calc.}})/\text{bandwidth}]^2 \quad (2)$$

addition, only  $R$  factors based on those cases where all expected bands are assigned were retained. No heed was paid to levels assigned as forbidden transitions. Calculated  $R$  factors were plotted as contour maps throughout polyparameter space in a similar manner to that described elsewhere<sup>6</sup> for figures of merit associated with magnetic properties.

The assignments, transition energies, and bandwidth factors assigned to  $[\text{NiL}_2\text{Cl}_2]$  are:  $A_2$  4 500 (1 500),  $A_1$  8 000 (1 500),  $B_1$  10 200 (1 500),  $A_2$  11 200 (1 100),  $A_2$  17 800 (1 200), and  $B_1$  18 100 (1 200)  $\text{cm}^{-1}$ . Several main conclusions emerged. First, no satisfactory agreement between the observed and calculated spectrum could be obtained for Racah parameter  $B$  greater than 550  $\text{cm}^{-1}$  (the free-ion value for  $\text{Ni}^{\text{II}}$  is  $B_0 = 1\,050\text{ cm}^{-1}$ ). For example, with  $B = 650$  or even 600  $\text{cm}^{-1}$ , the two highest energy bands are calculated as energetically too far separated from the remaining bands, a feature which cannot be removed by reasonable variation of any other parameter. Secondly, variations in the spin-orbit coupling parameter were essentially irrelevant so far as the spectrum is concerned. Thus  $B$  is determined from

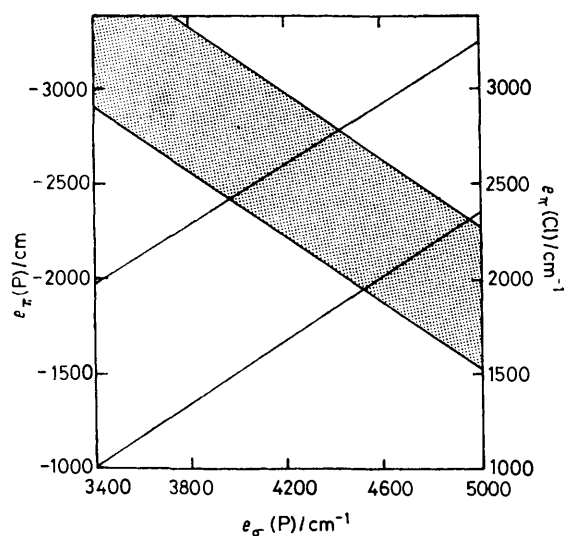


FIGURE 4 Spectral fitting regions for  $[\text{Ni}(\text{PPh}_3)_2\text{Cl}_2]$

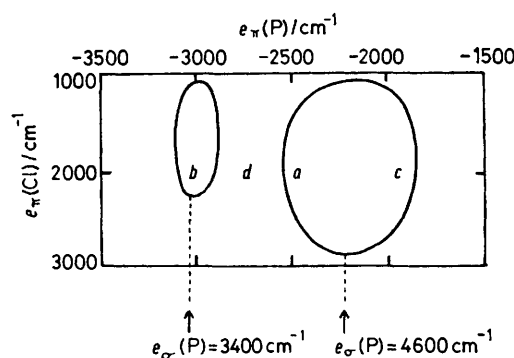


FIGURE 5 Correlation between  $e$  parameters which reproduce the observed spectrum of  $[\text{Ni}(\text{PPh}_3)_2\text{Cl}_2]$

the spectrum and  $\zeta$  from the magnetism. The behaviour of the spectral fit with respect to the ligand-field parameters can be summarized by the sketch in Figure 4. The contours surround regions of parameter space in which the mean spectral figure of merit  $R \geq 97\%$ . Rather little change in the diagram is evident for  $e_\sigma(\text{Cl})$  varying in the range 3 400–4 600  $\text{cm}^{-1}$ . On the other hand, the fitting region shifts smoothly in  $\pi$ -parameter space as  $e_\sigma(\text{P})$  varies, two cases being shown in Figure 5. Detailed quantitative agreement is shown in Table 2 for three points  $a$ ,  $b$ ,  $c$  corresponding to good spectral fits and one other,  $d$ , illustrating a worse parameter set. The correlation between parameter values yielding good spectral agreement in  $[\text{NiL}_2\text{Cl}_2]$  is illustrated in Figure 4. The relationship between  $e_\sigma(\text{P})$  and  $e_\pi(\text{P})$  is shown by the acceptable spectral fits lying in the hatched region. The unhatched area demonstrates the correlation between  $e_\sigma(\text{P})$  and  $e_\pi(\text{Cl})$ . The whole diagram varies insignificantly with respect to  $e_\sigma(\text{Cl})$ . We also note some tendency to favour higher  $e_\sigma$  values but this is based only on an increased frequency of very high spectral  $R$  factors for higher  $e_\sigma$  values. The trends shown in Figure 4 are maintained qualitatively for larger values of  $e_\sigma(\text{P})$ . For example, excellent fits to both the spectrum and the paramagnetism are possible for  $e_\sigma(\text{P})$  as large as 6 000

TABLE 2

Spectral fits for  $[\text{Ni}(\text{PPh}_3)_2\text{Cl}_2]$  corresponding to points labelled in Figure 5 ( $B = 550\text{ cm}^{-1}$ ,  $\zeta = 350\text{ cm}^{-1}$ )

Point	$e_\sigma(\text{P})$	$e_\sigma(\text{Cl})$	$e_\pi(\text{P})$	$e_\pi(\text{Cl})$
$a$	4 600	4 600	-2 500	2 000
$b$	3 400	3 800	-3 000	2 000
$c$	4 600	3 800	-2 000	2 000
$d$	3 400	3 400	-2 500	2 000

Species	Observed energy ( $\text{cm}^{-1}$ )	Calc. energies ( $\text{cm}^{-1}$ )			
		(a)	(b)	(c)	(d)
${}^3B_1$	18 100	18 600	18 200	17 300	17 100
${}^3A_2$	17 800	18 300	17 600	16 600	16 200
${}^3B_2$		16 400	15 300	15 800	14 600
${}^3A_2$	11 200	11 900	10 700	11 200	9 900
${}^3B_2$		9 800	9 200	9 200	8 200
${}^3B_1$	10 200	10 100	9 000	8 600	8 100
${}^3A_1$	8 000	7 200	6 700	6 700	6 100
${}^3A_2$	4 500	4 100	4 000	4 100	3 700
${}^3B_2$		3 100	2 900	3 600	3 000
${}^3B_1$		0	0	0	0
$R(\text{spectrum})$ :		98	96	95	87
$R(\text{magnetic})$ :		97	95	96	98

$k = 0.6$

$\text{cm}^{-1}$  [with  $e_o(\text{Cl})$  fixed, somewhat insensitively, at  $4\,000\ \text{cm}^{-1}$ ], provided we take  $e_n(\text{P})$  in the range  $-1\,000$  to  $-2\,000\ \text{cm}^{-1}$  and  $e_n(\text{Cl})$  as  $+2\,000$  to  $+3\,500\ \text{cm}^{-1}$ . This high value for  $e_n(\text{Cl})$  is some indication, but only slight in our view, that values for  $e_o(\text{P})$  lower than  $6\,000\ \text{cm}^{-1}$  are to be preferred. Altogether, there is rather little evidence for or against the notion of the phosphines acting as particularly strong  $\sigma$  donors in these systems.

Overall, therefore, fitting the polarized electronic spectrum of  $[\text{NiL}_2\text{Cl}_2]$  independently from the magnetic properties yields the same general conclusions so far as the ligand-field parameters are concerned, namely that  $e_n(\text{P})$  is negative and numerically greater than *ca.*  $1\,500\ \text{cm}^{-1}$  with  $e_n(\text{Cl})$  fairly large (*ca.*  $2\,000\ \text{cm}^{-1}$ ). Positive values for  $e_n(\text{P})$  cannot reproduce either observed susceptibilities or spectrum.

*Dichlorobis(triphenylphosphine)cobalt(II)*.—Similar procedures have been adopted for the magnetic and spectral properties of the chlorocobalt analogue. Fitting parameters to the magnetic properties alone again yields a wide range of possible  $e$  parameters although the response in the cobalt system was not as flat as in the nickel one. Positive  $e_n(\text{P})$  values are again rejected. The polarized single-crystal spectrum of  $[\text{CoL}_2\text{Cl}_2]$  has been reported by Simo and Holt<sup>8</sup> and the assignment in  $C_{2v}$  symmetry is shown in Table 3. The ground term is  $^4A_2$ , deduced from the electric dipole selection rule and the spectrum polarizations and is in agreement with that calculated by fitting the magnetic susceptibilities.

After some preliminary calculations in which  $e_n(\text{P})$  values in the range  $+1\,000$  to  $-3\,000\ \text{cm}^{-1}$  were considered, detailed examination of the following parameter ranges was made:  $e_o(\text{P})$   $3\,400$ – $4\,000$ ,  $e_o(\text{Cl})$   $3\,400$ – $4\,200$ ,  $e_n(\text{P})$   $-500$  to  $-1\,500$ ,  $e_n(\text{Cl})$   $1\,500$ – $3\,000\ \text{cm}^{-1}$ . The interelectron repulsion parameter  $B$  was fixed from the spectrum as *ca.*  $575\ \text{cm}^{-1}$  ( $B_0 = 1\,120\ \text{cm}^{-1}$ ) and the spin-orbit coupling parameter was fixed from the magnetism as  $\zeta$  *ca.*  $500\ \text{cm}^{-1}$  ( $\zeta_0 = 515\ \text{cm}^{-1}$ ). The value of  $k$  was insensitively fixed from the susceptibilities to lie in the range  $0.5$ – $0.8$ . Within the given ranges for the ligand-field parameters, combinations with spectral  $R$  factors less than  $90\%$  and/or magnetic  $R$  factors less than  $85\%$  were rejected. The remaining fitting combinations can be summarized as follows. No satisfactory agreement with the spectrum is possible for  $e_n(\text{P})$  values outside the range  $-1\,000$  to  $-2\,000\ \text{cm}^{-1}$ , or for  $e_n(\text{Cl})$  outside the range  $2\,000$ – $3\,000\ \text{cm}^{-1}$ . Within these ranges, the correlations between acceptable  $e$  parameters are shown in Table 4. Values of  $e_n(\text{Cl})$  and

TABLE 3  
Spectrum<sup>8</sup> of  $[\text{Co}(\text{PPh}_3)_2\text{Cl}_2]$

Polarization	Assignment	Transition energy ( $\text{cm}^{-1}$ )	'Bandwidth' ( $\text{cm}^{-1}$ )
$x$	$B_2$	6 400	500
$z$	$A_2$	8 000	600
$y$	$B_1$	10 700	800
$y$	$B_1$	13 600	500
$z$	$A_2$	15 800	500
$x$	$B_2$	16 700	500

TABLE 4

Correlations of  $e$  parameters for simultaneous good spectral and good magnetic fits for  $[\text{Co}(\text{PPh}_3)_2\text{Cl}_2]$

$e_o(\text{P})$	$e_o(\text{Cl})$		
	3 400	3 800	4 200
3 800	2 000		
4 200	( $e$ ) -1 500		
4 600	2 500	2 000	2 500
	-1 500	-1 000	-1 000
	2 800	2 500	3 000
	( $g$ ) -1 500	-1 000	( $f$ ) -1 000

TABLE 5

Comparison of observed and calculated spectra for  $[\text{Co}(\text{PPh}_3)_2\text{Cl}_2]$  corresponding to the parameter values given in Table 4. Calculated  $^4A_2 \rightarrow ^4A_1$  (forbidden) bands have been omitted

Species	Obs. spectrum ( $\text{cm}^{-1}$ )	Calc. spectra ( $\text{cm}^{-1}$ )		
		( $e$ )	( $f$ )	( $g$ )
$\rightarrow ^4B_2$	16 700	16 700	16 700	16 800
$\rightarrow ^4A_2$	15 800	15 600	16 700	16 800
$\rightarrow ^4B_1$	13 600	13 000	12 500	13 400
$\rightarrow ^4B_1$	10 700	10 600	10 500	11 200
$\rightarrow ^4A_2$	8 000	7 900	7 600	8 200
$\rightarrow ^4B_2$	6 400	6 400	6 300	6 800
$R(\text{spectrum})$		97	90	97
$R(\text{magnetic})$		91	86	89

$e_n(\text{P})$  are shown in the Table at the top right-hand side and bottom left-hand side respectively. All entries correspond to spectral  $R$  factors greater than  $90\%$  and magnetic  $R$  factors greater than  $85\%$ . Two trends may just be deduced from the Table: (*i*) larger  $e_n(\text{P})$  values seem to be favoured; (*ii*) larger  $e_n(\text{Cl})$  values are associated with numerically larger  $e_n(\text{P})$  values. Detailed agreement between observed and calculated transition energies (all being correctly assigned) are shown in Table 5 for the three points  $e, f, g$  in Table 4.

Overall, therefore, independent fitting of the spectral and magnetic properties of  $[\text{CoL}_2\text{Cl}_2]$  and  $[\text{NiL}_2\text{Cl}_2]$  yields similar results. For the cobalt system no fit is possible for  $e_n(\text{P})$  less negative than  $-1\,000\ \text{cm}^{-1}$ , the magnetic  $R$  factors deteriorating rapidly as  $e_n(\text{P})$  approaches zero or positive values. We may discern a qualitative difference between these two systems in that  $|e_n(\text{P})| < e_n(\text{Cl})$  for the cobalt molecule and  $|e_n(\text{P})| \gtrsim e_n(\text{Cl})$  for the nickel one. Less clear is that  $e_o(\text{P}) \gtrsim e_o(\text{Cl})$  in the cobalt system but no relationship is established in the nickel one. In general,  $e_o$  values have not been well determined for these complexes. For the purposes of comparison, a typical choice of  $e_n$  values for good spectral and good magnetic fit would be  $e_n(\text{P})$   $-2\,500$  and  $-1\,000\ \text{cm}^{-1}$  for the nickel and cobalt systems, respectively, while  $e_n(\text{Cl})$  takes the value  $+2\,000\ \text{cm}^{-1}$  for both.

*Dibromobis(triphenylphosphine)nickel(II)*.—As for the chloro-analogue, good fits to the magnetic susceptibility alone define a flat region of parameter space bounded by  $e_n(\text{P})$   $-1\,000$  to  $-3\,000\ \text{cm}^{-1}$  and  $e_n(\text{Br})$   $+1\,000$  to  $+3\,000\ \text{cm}^{-1}$ ;  $\zeta$  *ca.*  $300\ \text{cm}^{-1}$ ;  $k$   $0.5$ – $0.8$ ;  $B = 550\ \text{cm}^{-1}$ . Huddersman<sup>10</sup> has reported the diffuse-reflect-

TABLE 6

Spectral fits for  $[\text{Co}(\text{PPh}_3)_2\text{Br}_2]$  corresponding to parameter values given in Table 7

Polarization	Assignment	Obs. energy <sup>a</sup> (cm <sup>-1</sup> )	Calc. energy (cm <sup>-1</sup> )
<i>x</i>	<sup>4</sup> B <sub>2</sub>	15 900	15 800
<i>z</i>	<sup>4</sup> A <sub>2</sub>	14 900	14 900
<i>y</i>	<sup>4</sup> B <sub>1</sub>	13 500	12 600
<i>y</i>	<sup>4</sup> B <sub>1</sub>	9 700	9 300
<i>z</i>	<sup>4</sup> A <sub>2</sub>	7 600	7 100
<i>x</i>	<sup>4</sup> B <sub>2</sub>	6 000	5 900
			5 400
			3 600
			3 500
	<sup>4</sup> A <sub>2</sub>	0	0

ance spectrum for which no assignment is directly possible. It is, however, closely similar to the spectrum of  $[\text{NiL}_2\text{Cl}_2]$  except that the two higher energy bands lie much closer in energy to the majority of the transitions. Transition peaks occur at 4 000, 8 800, 10 900, 14 900, and 16 800 cm<sup>-1</sup>. We have fitted these peaks without assignment (although the band ordering is the same as that observed for the chloro-system), using 'bandwidth' factors of 1 200, 1 000, 1 000, 1 200, and 1 200 cm<sup>-1</sup> respectively. Overall, good agreement with the spectrum ( $R \gtrsim 96\%$ ) and with the crystal susceptibilities ( $R \gtrsim 91\%$ ) is possible within the ranges:  $e_\pi(\text{P}) -1 000$  to  $-2 000$  cm<sup>-1</sup>;  $e_\pi(\text{Br}) +1 000$  to  $2 000$  cm<sup>-1</sup>;  $e_\sigma(\text{P})$  and  $e_\sigma(\text{Br})$  ca. 4 000 cm<sup>-1</sup> each, but insensitively fixed. In comparison with  $[\text{NiL}_2\text{Cl}_2]$ , we find  $e_\pi(\text{Br}) < e_\pi(\text{Cl})$  and  $|e_\pi(\text{P})_{\text{Br}}| \lesssim |e_\pi(\text{P})_{\text{Cl}}|$ .

*Dibromobis(triphenylphosphine)cobalt(II)*.— Tomlinson *et al*<sup>9</sup> have reported the single-crystal polarized transmission spectrum of this system. Again, six bands have been identified and are readily assigned using electric dipole selection rules (Table 6). We have quantitatively reproduced these spectral energies and assignments simultaneously with the principal crystal susceptibilities over the whole experimental temperature range, as was done for the previous three complexes. We find that in this case various  $e$  parameters are somewhat more sensitively established, except that the 'best-fit' values vary significantly with  $\zeta$ , the spin-orbit coupling coefficient. While  $\zeta$  was fairly well defined for the nickel complexes, a wide range is possible for  $[\text{CoL}_2\text{Br}_2]$ , acceptable magnetic and spectral fits being found for  $\zeta$  in the range 300–500 cm<sup>-1</sup>. the strongest correlation is observed between  $\zeta$  and  $e$  values, larger  $\zeta$  being associated with smaller  $e_\sigma$ . The final 'best-fit' parameter set (Table 7) was taken to reproduce the experimental data (Tables 1 and 6) and was chosen with  $\zeta = 500$  cm<sup>-1</sup> by

comparison with the chlorocobalt system and also because trends in  $e$  parameters for all four complexes are revealed for this higher value. The value of the orbital reduction factor  $k$  was again insensitively fixed within the range 0.5–0.8.

*Conclusions*.—The most general and obvious conclusion to be derived from the independent fitting of crystal magnetic data and crystal or powder spectral data of all four complexes  $[\text{ML}_2\text{X}_2]$  is that fairly large positive  $e_\pi$  parameters for the halogen atoms are associated with fairly large negative  $e_\pi$  values for triphenylphosphine. In its simplest and oldest form, the angular overlap model (a.o.m.) envisaged the  $e$  parameters as directly related to the degree of metal–ligand overlap, so far as the antibonding metal functions are concerned, and indeed the approach was named on that basis.<sup>13</sup> However, the criterion of overlap defining the  $e$  parameters does not emerge from first principles and we argue elsewhere<sup>14</sup> that, while ligand-field theory as a procedure and the a.o.m. as a formalism are well founded in quantum chemistry, correlations of the magnitude of  $e$  parameters and overlap within the same symmetry type depend upon a notion of empirical calibration. Thus, as a matter of experience, essentially zero  $e_\pi$  parameter values are observed with ammonia and other amine ligands, for example, in support of the idea that  $e$  parameters are proportional to some power (in the most elementary theory, to the square) of the metal–ligand overlap integral. Our recent treatment<sup>14</sup> of ligand-field theory from first principles, however, fails to suggest why such a relationship *must* emerge. Nevertheless, experience with the a.o.m. does tend to indicate that vanishing  $e_\pi$  parameters are associated with non- $\pi$ -bonding ligands so that the sign of any empirical  $e_\pi$  value should relate to donor or acceptor properties. However, it could be argued that such confidence is largely based upon evidence from ligands with nitrogen-donor atoms. Altogether therefore, we do not consider that enough is yet known about angular overlap parameters to allow the claim that a zero value for  $e_\pi(\text{P})$  necessarily implies the lack of any  $\pi$  interaction. However, the arguments developed elsewhere<sup>14</sup> suggest that if this is not the case the most likely conclusion to be drawn is that positive  $e_\pi$  parameters could occasionally be associated with no  $\pi$  bonding. It is extremely unlikely that the large negative values for  $e_\pi(\text{P})$  determined in the present systems can be associated with anything but a  $\pi$ -accepting role of the phosphines. This conclusion is supported by the *relative*  $e_\pi$  values found for the phosphine and halogen ligands in these systems and there seems to be a

TABLE 7

'Best-fit' parameter sets chosen to reproduce the crystal magnetism and spectra

Parameter	$[\text{Ni}(\text{PPh}_3)_2\text{Cl}_2]$	$[\text{Ni}(\text{PPh}_3)_2\text{Br}_2]$	$[\text{Co}(\text{PPh}_3)_2\text{Cl}_2]$	$[\text{Co}(\text{PPh}_3)_2\text{Br}_2]$
$B/\text{cm}^{-1}$	550	550	575	575
$\zeta/\text{cm}^{-1}$	350	300	500	500
$e_\sigma(\text{P})/\text{cm}^{-1}$	4 500	4 000	4 000	3 500
$e_\pi(\text{P})/\text{cm}^{-1}$	-2 500	-1 500	-1 000	-1 000
$e_\sigma(\text{X})/\text{cm}^{-1}$	4 500	4 000	3 500	3 500
$e_\sigma(\text{X})/\text{cm}^{-1}$	2 000	1 500	2 000	1 500
$k$	0.6	0.6	0.6	0.6

strong indication that donation by the halogens is encouraged by  $\pi$  acceptance by the phosphines in line with the electroneutrality principle.

In Table 7 we collect the 'best-fit' parameter sets for all four complexes chosen to reproduce the crystal magnetism in Table 1 and the experimental spectra discussed earlier. Orbital diagrams corresponding to these parameter sets (but with vanishing  $\zeta$  values for simplicity) are similar for all four complexes as expected from the parameter values in Table 7. That for  $[\text{NiL}_2\text{Cl}_2]$  is shown in Figure 6(a) together with corres-

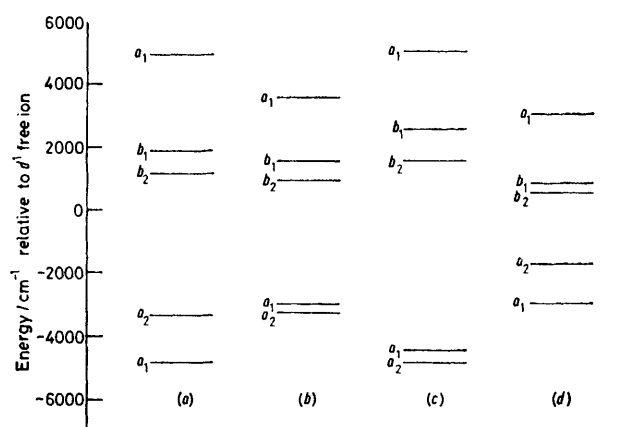


FIGURE 6 Orbital-splitting diagrams calculated with the  $e$  parameter values given in Table 7 and without spin-orbit coupling

ponding orbital diagrams calculated for: (b) no  $\pi$  contribution from phosphorus or chlorine; (c) no  $\pi$  bonding from the chlorines; (d) no  $\pi$  interaction from the phosphines. From Figure 6(a) we observe that the average energy of the components ( $a_1 + b_1 + b_2$ ) from  $t_2(T_d)$  minus the average energy of the components ( $a_1 + a_2$ ) from  $e(T_d)$  is some  $6\,800\text{ cm}^{-1}$ , corresponding to  $\Delta_{\text{tet}}$ . Comparing diagrams 6(a) and 6(d), we note that the  $\pi$ -acceptor role of the phosphines contributes *ca.*  $2\,900\text{ cm}^{-1}$  to the  $\Delta_{\text{tet}}$  value. The trends in  $e_\pi$  values appear well established while uncertainties in the ranges for  $e_\sigma$  are such that no conclusion beyond their similarity over the series can be made. We observe that the phosphines are less good  $\pi$  acceptors in the cobalt species (compared

with the nickel ones) and we interpret this as reflecting an enhanced metal-donor property for the nickel atoms, following the addition of one more electron into the  $d$ -orbital stack as cobalt is replaced by nickel.

Recent estimates<sup>15</sup> of  $e_\sigma$  and  $e_\pi$  values in tetrahedral  $[\text{CuCl}_4]^{2-}$  and  $[\text{CuBr}_4]^{2-}$  ions suggest that both parameters decrease on replacing Cl by Br. The same result tends to emerge from the present study in that  $e_\pi(\text{Br}) \leq e_\pi(\text{Cl})$ .

When fitting the spectra of these complexes we were forcibly struck by the low values required for the Racah  $B$  values, several unsuccessful attempts having been made to reproduce spectral transition energies with smaller nephelauxetic effects. Within a molecular-orbital framework the large nephelauxetic effects observed in these complexes seems readily understandable within the notion of delocalization of the spectral electrons onto the ligands involved in considerable  $\pi$  bonding with the central metal. Participation of empty phosphorus  $d_\pi$  orbitals would appear especially effective here.

We thank the University of New South Wales for study leave to D. J. P.

[8/2040 Received, 23rd November, 1978]

#### REFERENCES

- R. Mason and D. W. Meek, *Angew. Chem. Internat. Edn.*, **1978**, **17**, 183.
- M. Gerloch, *Progy. Inorg. Chem.*, in the press.
- L. M. Venanzi, *J. Chem. Soc.*, **1958**, 719.
- G. Garton, D. E. Henn, H. M. Powell, and L. M. Venanzi, *J. Chem. Soc.*, **1963**, 3625.
- J. A. J. Jarvis, R. H. B. Mais, and P. G. Owston, *J. Chem. Soc. (A)*, **1968**, 1473.
- D. A. Cruse and M. Gerloch, *J.C.S. Dalton*, **1977**, 152.
- R. J. Fereday, B. J. Hathaway, and R. J. Dudley, *J. Chem. Soc. (A)*, **1970**, 571.
- C. Simo and S. Holt, *Inorg. Chem.*, **1968**, **7**, 2655.
- A. A. G. Tomlinson, G. Bellitto, O. Piovesana, and C. Furlani, *J.C.S. Dalton*, **1972**, 350.
- K. D. Huddersman, Ph.D. Thesis, London University, **1977**.
- M. Gerloch and R. F. McMeeking, *J.C.S. Dalton*, **1975**, 2443.
- M. Gerloch and I. Morgenstern, *Inorg. Chem.*, in the press.
- M. Gerloch and R. C. Slade, 'Ligand Field Parameters,' Cambridge University Press, **1973**.
- M. Gerloch, J. H. Harding, and R. G. Woolley, in preparation.
- D. A. Cruse and M. Gerloch, *J.C.S. Dalton*, **1977**, 1617.